Available online at www.sciencedirect.com

SciVerse ScienceDirect

Ceramics International 39 (2013) 6175–6182

CERAMICS INTERNATIONAL

www.elsevier.com/locate/ceramint

Electrochemical and structural study of $Ce_{0.8}Sm_{0.2-x}La_xO_{1.9}$ electrolyte materials for SOFC

Massoud Kahlaoui[a,*], Abdelwaheb Inoubli[a], Sami Chefi[a], Abdessalem Kouki[a], Adel Madani[a,b], Chaabane Chefi[a]

[a]Laboratoire de Physique des Matériaux, Faculté des Sciences de Bizerte, Université de Carthage, Zarzouna 7021, Tunisia
[b]College of Applied Sciences, Department of Physics, Umm Al Qura University, Makkah, Saudi Arabia

Received 13 December 2012; received in revised form 11 January 2013; accepted 12 January 2013
Available online 23 January 2013

Abstract

$Ce_{0.8}Sm_{0.2-x}La_xO_{1.9}$ powders, denoted as La_xSDC (for $x=0$, 0.01, 0.03, 0.05, 0.07 and 0.1), were synthesized via the mechanical milling reaction method. The La^{3+} doping content has a remarkable influence on structural and electrical properties. The phase identification and morphology were studied by X-ray diffraction (XRD) and scanning electron microscopy (SEM). Lattice parameters were calculated by the Rietveld method. It was observed that the lattice parameter values in $Ce_{0.8}Sm_{0.2-x}La_xO_{1.9}$ systems obey Vegard's law. The pellets were then sintered at 1500 °C in air for 7 h. The relative densities of these pellets were over 93.7%.The electrical conductivity was studied using two-probe impedance spectroscopy and results showed that the conductivity of $Ce_{0.8}Sm_{0.2-x}La_xO_{1.9}$ first increased and then decreased with La dopant content x. Results also showed that $Ce_{0.8}Sm_{0.17}La_{0.03}O_{1.9}$ had the highest electrical conductivity, $\sigma_{700\,°C}$ equal to 3.8×10^{-2} Scm^{-1} and an activation energy equal to 0.77 eV. It was therefore concluded that co-doping with the appropriate amount of La can further improve the electrical properties of ceria electrolytes.

Keywords: SOFC; Mechanical milling process; Co-doped ceria; Impedance spectroscopy

1. Introduction

Taking into account its higher ionic conductivity at much lower temperatures compared to YSZ and its good compatibility with electrodes [1–3], doped ceria has been considered a better candidate for use as an electrolyte in intermediate temperature solid oxide fuel cells (IT-SOFC). Among the currently used doped ceria are those with general formula $Ce_{1-x}M_xO_{2-\delta}$ for M = Gd^{3+}, Sm^{3+}, Y^{3+}, La^{3+},Nd^{3+}, Eu^{3+}, Sr^{2+}, Ca^{2+} [3–13], etc. These materials have remarkable properties in terms of structural, electrochemical and thermal stability. Dopant cations mentioned above introduced an oxygen vacancy in the lattice as charge compensating defects and increased the ionic conductivity. However, when exposed to the reducing atmosphere, their electrical conduction requires co-doping to obtain acceptable performances and to improve their electrical properties. So far, some co-doped ceria-based electrolytes, such as $Ce_{0.8}Ca_{0.2-x}Sm_xO_y$ [14], $Ce_{1-x}(Sm_{0.5}Nd_{0.5})_xO_\delta$ [15], $Ce_{0.8}Gd_{0.2-x}Nd_xO_{2-\delta}$ [16], $Ce_{0.8}Y_{0.2-x}Sr_xO_{2-\delta}$ [17], $Ce_{0.8}Gd_{0.2-x}Y_xO_{2-\delta}$ [18] and $Ce_{0.8-x}Sm_{0.2}Ca_xO_{2-\delta}$ [19], have been studied. Since $Ce_{0.8}Sm_{0.2}O_{1.9}$, $Ce_{0.8}Gd_{0.2}O_{1.9}$ and $Ce_{0.8}La_{0.2}O_{1.9}$ were found to have the highest conductivity [20], Sm and La co-doped ceria are probably better electrolytes. However, there is still a lack of research results on these materials.

In this work, Sm^{3+} and La^{3+} co-doped ceria materials were prepared and characterized for the first time. The effect of co-doping on structure and conductivity was then studied and compared to singly-doped ceria. Highly conductive electrolytes were found. The aim was to develop new ceria-based electrolyte materials to further improve their ionic conductivity.

2. Experimental

$Ce_{0.8}Sm_{0.2-x}La_xO_{1.9}$ electrolytes ($x=0$, 0.01, 0.03, 0.05, 0.07, and 0.1) were synthesized using the mechanical

*Corresponding author. Tel.: +216 72591906; fax: +216 72590566.
E-mail address: kahlaouimessaoud@yahoo.fr (M. Kahlaoui).

0272-8842/$ - see front matter © 2013 Elsevier Ltd and Techna Group S.r.l. All rights reserved.
http://dx.doi.org/10.1016/j.ceramint.2013.01.036

milling reaction method. All starting materials used were highly pure: cerium oxide (CeO_2), 99.99% (Aldrich), samarium oxide (Sm_2O_3), 99.99% (Aldrich), and lanthanum oxide (La_2O_3), 99.99% (Aldrich). The bibliographic studies [17,21] can provide some information on this type of synthesis. However, the experimental protocol generally requires many stages of calcinations and crushing to obtain the desired phase. Precursors in stoichiometric amounts were mixed and ground in ethanol for about 7 h at 200 rpm using zirconium (ZrO_2) balls in a planetary mill (Retsch PM 200). When dried, the resulting powders were then treated at 1200 °C for 2 h. The as-synthesized powders were milled again with ethanol for 5 h at 200 rpm, dried and calcined at 1350 °C for 5 h to give the desired phase. Finally, grinding the synthesized powders (at 400 rpm/40 min) gave a better sinterability.

The phase composition of the obtained La_xSDC powders was identified using X-ray diffraction (XRD) with a Bruker D8 Advance Germany diffractometer which uses CuKα monochromatic radiation at room temperature. The crystalline phase and cell parameters were fitted with the PANalytical X'Pert High Score Plus program using the Rietveld method. The average crystallite size (D) was also defined by using the Scherrer formula: $D = 0.9\lambda/\beta\cos\theta$. The morphology and microstructure of La_xSDC were observed with a scanning electron microscope (SEM, JEOL.JSM-5400). A laser size analyzer (Malvern Mastersizer 2000) was used to perform particle size distribution measurement. The dried powders were ground in an agate mortar and then pressed to 5 MPa into cylindrical pellets (12–13 mm in diameter and 0.8–1.5 mm in thickness). The pellets were then sintered at 1500 °C in air for 7 h with a heating and cooling rate of 200 °C/h. Experimental densities of the sintered pellets were determined using a pycnometer with distilled water and were then compared to the theoretical values determined from the lattice parameters.

Electrochemical impedance spectra (EIS) were obtained using a Hewlett–Packard HP 4192 Analyzer. Impedance measurements were carried out in an open circuit using two electrode configurations with a signal amplitude of 50 mV and a frequency band ranging from 5 Hz to 13 MHz. Both pellet surfaces were coated with silver pastes to act as electrodes and platinum wires attached to the electrodes were used as current collectors. All these measurements were performed at equilibrium potential as a function of temperature (250–700 °C)

In order to obtain the bulk, grain boundary and total ionic conductivity, the data obtained was analyzed using the equivalent circuit of the Zview software.

3. Results and discussion

3.1. Crystal structure

Fig. 1(a) shows the XRD patterns of the $Ce_{0.8}Sm_{0.2-x}La_xO_{1.9}$ (La_xSDC) solid solutions prepared by the mechanical milling reaction method and calcined at 1350 °C for 5 h. It can be seen that all powders were single phased with a cubic fluorite structure and space group Fm3m (JCPDS powder diffraction file no. 34-0394). No other peaks attributable to impurities or other phases were detected. The structural refinement of the SDC was carried out using the Rietveld method. The fitting of the XRD pattern of the SDC is shown in Fig. 2.

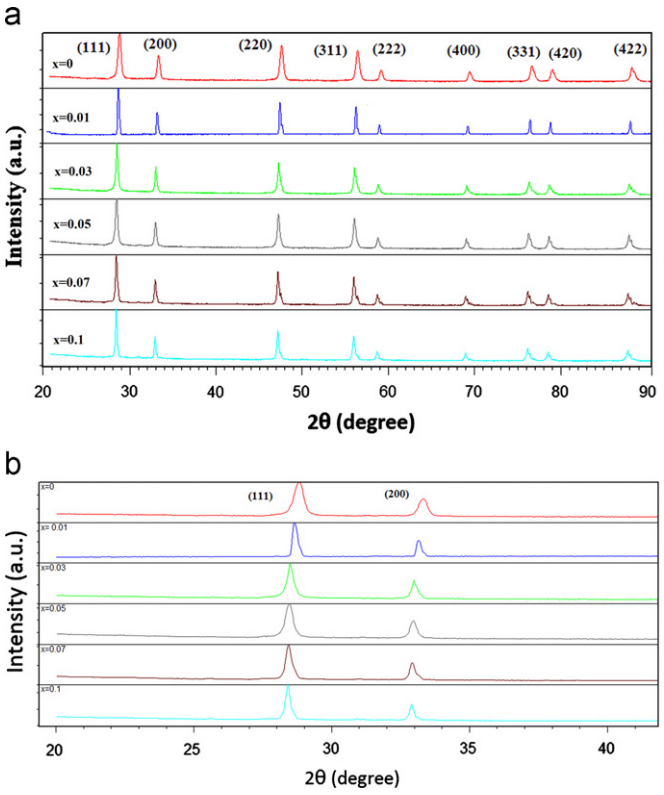

Fig. 1. (a) X-ray diffraction patterns of synthesized $Ce_{0.8}Sm_{0.2-x}La_xO_{1.9}$ powders calcined at 1350 °C. (b) Shift of (111) and (200) XRD peaks for $Ce_{0.8}Sm_{0.2-x}La_xO_{1.9}$ with La content.

Final R-goodness factors were $R_p = 4.17$, $R_{wp} = 5.75$, $R_e = 3.74$ and χ^2 (chi^2) $= 2.37$.

The crystallite sizes (D_{XRD}) of the La_xSDC powders, calculated by the Scherrer formula, were found to be between 44.5 and 482 nm (Table 1).

It was also found that the position of the diffraction peaks moved towards lower angles, with x ranging from 0 to 0.1 as shown in Fig. 1(b).This is due to the decrease in ionic radius in the following order: La^{3+} (1.15 Å) > Sm^{3+} (1.08 Å) > Ce^{4+} (0.97 Å); thus, the substitution of Ce^{4+} with La^{3+} and Sm^{3+} in the CeO_2 lattice would enlarge said crystal lattice.

Fig. 3 shows the relationship between the lattice parameter for $Ce_{0.8}Sm_{0.2-x}La_xO_{1.9}$ and the doping content. This can be expressed as $a(x) = 0.1738x + 5.4449$. As it can be seen, the lattice parameter increases linearly with increasing lanthanum content, which is found to obey Vegard's rule [15,22]. Therefore, the increased lattice parameter testifies that samarium and lanthanum are indeed in

the ceria crystal lattice. These results are similar to previous work [23,24].

3.2. Microstructure

The sintered density was determined using the Archimedes principle which was described in our previous work [25].

The equation used for calculating the theoretical density (D_C) is as follows:

$$D_{\text{theo}} = \frac{4xM_{\text{La}} + 4(0.2-x)M_{\text{Sm}} + 3.2M_{\text{Ce}} + 7.6M_{\text{O}}}{N_{\text{A}}[a(x)]^3} \quad (1)$$

where M_{La}, M_{Sm}, M_{Ce} and M_{O} represent the atomic weights of doping cations, cerium and oxygen, N_{A} is the Avogadro number and a is the calculated lattice parameter.

Table 1 summarizes the calculated density (D_c), the measured sintered density (D_m) and the relative density (D_m/D_c) of the $Ce_{0.8}Sm_{0.2-x}La_xO_{1.9}$ series. It can be seen that the measured densities for all sintered samples were between 93.7% and 95.9%, relative to the theoretical value. As shown in Table 1, it was necessary to submit all sample powders to ultrasound vibrations for 20 min in order to dissociate the largest agglomerates. A monomodal particle distribution was then obtained with the width of the size distribution (S) lying between 1.07 and 1.98 μm.

$$S = \frac{d_{90} - d_{10}}{d_{50}} \quad (2)$$

where d_{10}, d_{50} and d_{90} are the particle sizes when the accumulative distributions are10%, 50% and 90% respectively. The powders have a severe agglomeration and broad size distribution as shown in Fig. 4. The SEM micrograph of La_xSDC (x=0–0.1) samples sintered at 1500 °C for 7 h is

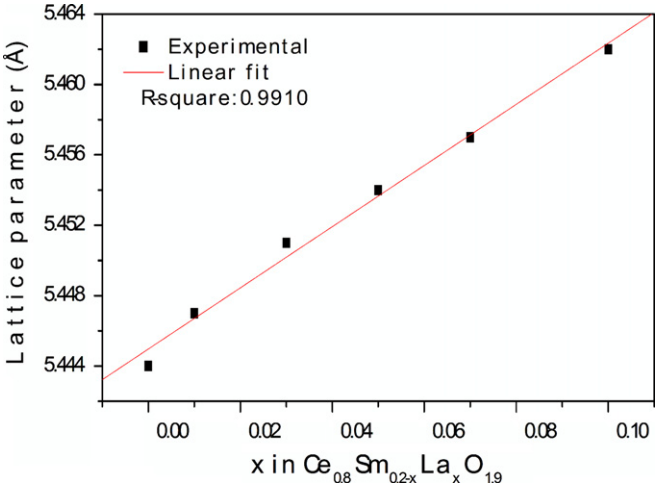

Fig. 3. Dependence of the lattice constant on the La content in co-doped ceria electrolytes.

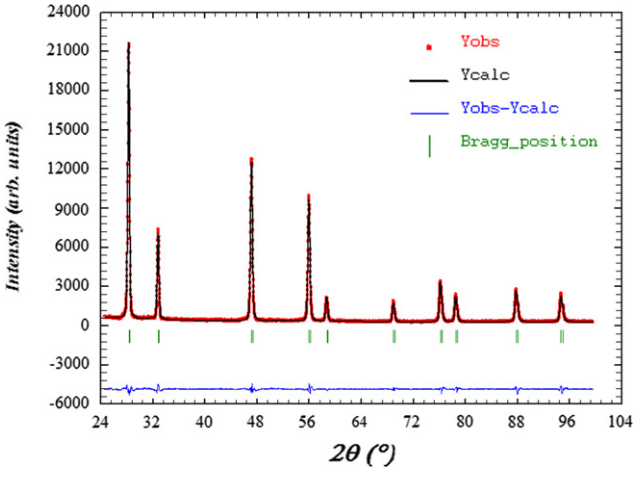

Fig. 2. Rietveld analysis of the $Ce_{0.8}Sm_{0.2}O_{1.9}$ doped ceria fluorite. Peak position and the differences between observed and calculated profiles are shown.

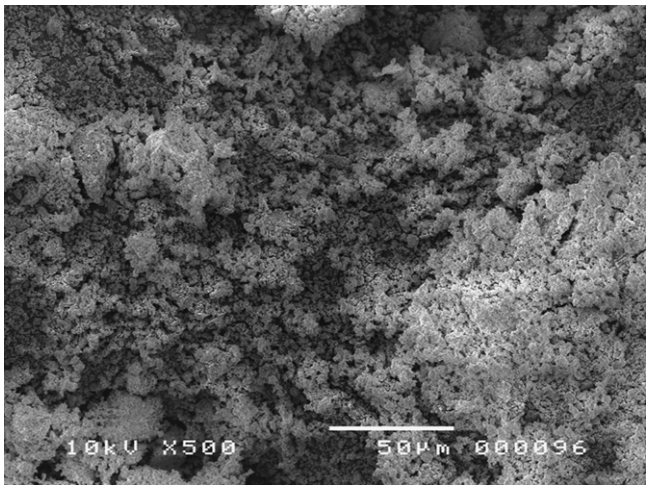

Fig. 4. SEM of prepared $Ce_{0.8}Sm_{0.2}O_{1.9}$ powder calcined at 1350 °C for 5 h.

Table 1
Measured and calculated properties of the $Ce_{0.8}Sm_{0.2-x}La_xO_{1.9}$ series.

Composition	D_{XRD} (nm)	S	a (Å)	D_c (g cm^{-3})	D_m (g cm^{-3})	D_m/D_c (%)
SDC	44.5	1.98	5.444	7.076	6.69	94.5
$La_{0.01}$SDC	120.6	1.42	5.447	7.064	6.71	95.0
$La_{0.03}$SDC	482.1	1.07	5.451	7.043	6.72	95.4
$La_{0.05}$SDC	69.5	1.42	5.454	7.022	6.72	95.7
$La_{0.07}$SDC	240.1	1.31	5.457	7.001	6.64	94.8
$La_{0.1}$SDC	372.5	1.17	5.462	6.968	6.53	93.7

shown in Fig. 5. The micrograph shows that the samples of SDC and $La_{0.01}$SDC (Fig. 5a–b) were found to be very porous, the pores of which were continuous and open. In contrast, the $La_{0.03}$SDC and $La_{0.05}$SDC samples (Fig. 5c–d) were denser. The grains were very close to each other and the grain boundary was very clear, which is consistent with the relative density values given in Table 1. As for the $La_{0.07}$SDC and $La_{0.1}$SDC samples (Fig. 5e–f), it can be seen that said grains have a non-uniform size and that pinholes appear at grain boundaries. However, these pinholes were attributed to the oxygen release reaction, according to Li et al. and Yao et al. [16–26]. The average grain size for all samples is lower than 3.5 μm.

3.3. Electrical characterization

AC impedance spectroscopy is widely employed to obtain information related to the electrical behavior of grains, grain boundaries and electrode response. A typical impedance spectrum measured at 300 °C under air for the La_xSDC ($x = 0$–0.1) pellets with equivalent circuit is illustrated in Fig. 6. The data of the electrochemical impedance spectra (EIS) was fitted to the equivalent circuit of the R_s (R_b CPE_b) (R_{gb} CPE_{gb}) (R_{el} CPE_{el}) type shown in Fig. 6, where R_s is the ohmic resistance of the La_xSDC electrolyte and the three series connected elements (R//CPE). R is resistance and CPE is a constant phase element representing time-dependent capacitive elements. The first component, (R_b CPE_b), appears as a semi-circle in the high-frequency region, the second one, (R_{gb} CPE_{gb}), as a semi-circle in the medium-frequency region and the third one, (R_{el} CPE_{el}), as an incomplete semi-circle in the low-frequency region. This pattern can be attributed to the grains, the grain boundaries and the electrochemical response of the silver electrode, respectively. The amplitude of this arc is thermally dependent and increases with decreasing La proportion.

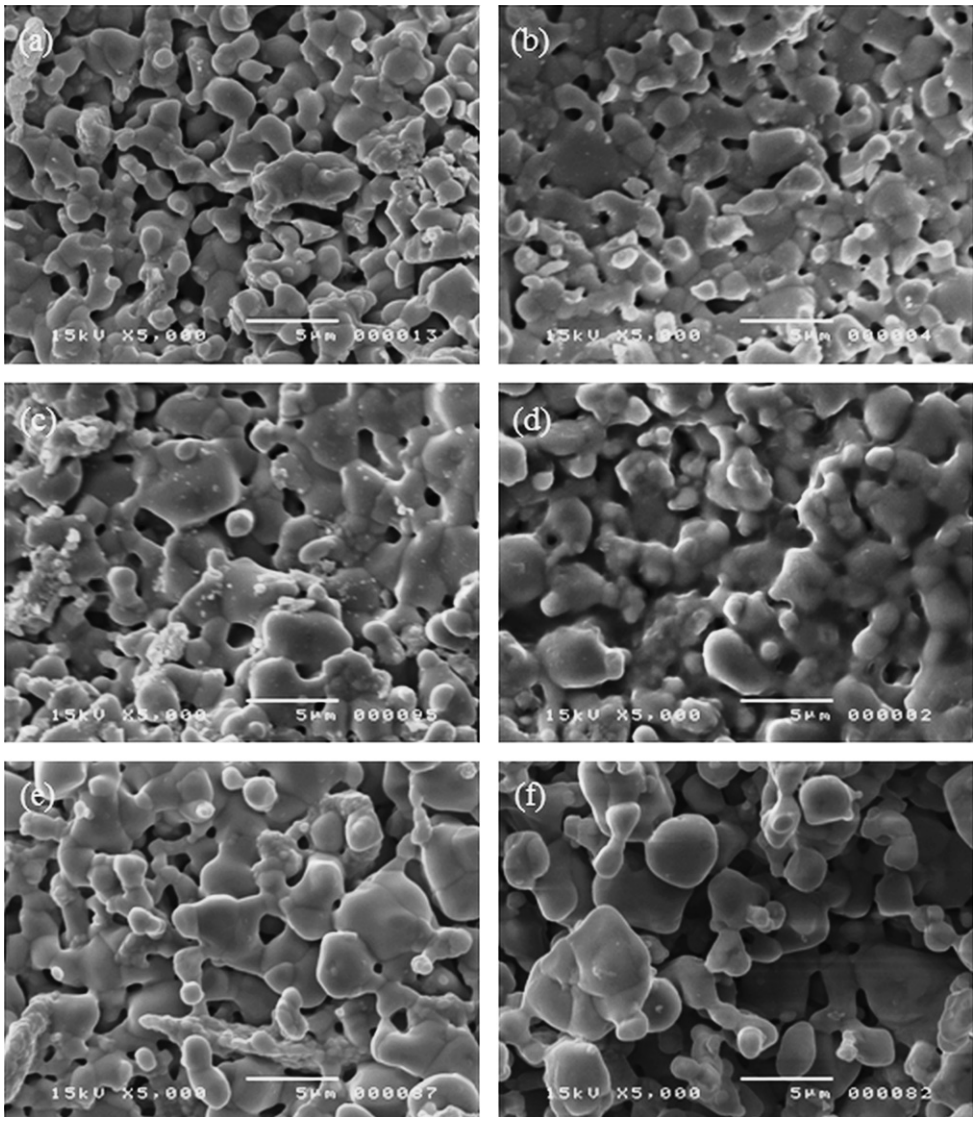

Fig. 5. SEM photographs of the samples sintered at 1500 °C for 7 h in air: (a) SDC, (b) $La_{0.01}$SDC, (c) $La_{0.03}$SDC, (d) $La_{0.05}$SDC, (e) $La_{0.07}$SDC and (f) $La_{0.1}$SDC.

For a pellet with thickness, d, and section area, S, the total, bulk and grain boundary conductivities were calculated using the following relation:

$$\sigma_i = \frac{1}{R_i} \times \frac{d}{S} \tag{3}$$

where R_i ($i=b$, gb, tot) is the resistance obtained from impedance spectra. In this work, the total conductivity values that will be presented are the sum of the bulk and grain boundary conductivities which are calculated from this equation:

$$\frac{1}{\sigma_{tot}} = \frac{1}{\sigma_b} + \frac{1}{\sigma_{gb}} \tag{4}$$

Activation energies (E_a) were obtained by fitting the conductivity data to the Arrhenius relation for thermally-activated conduction, which is calculated using the following equation:

$$\sigma = \frac{\sigma_0}{T} \exp\left(-\frac{E_a}{kT}\right) \tag{5}$$

where σ, σ_0, E_a, k and T are the conductivity, pre-exponential factor, activation energy, Boltzmann constant and absolute temperature, respectively.

Substitution of the ceria by rare-earth and other trivalent and divalent oxides produces oxygen vacancies in the lattice giving rise to ionic conduction [27]. As given by Eqs. (6) and (7), written in the Kroger–Vink notation, the addition of lanthanum and samarium to CeO_2 induce the formation of oxygen vacancies

$$La_2O_3 \xrightarrow{2CeO_2} 2La'_{Ce} + V_{\ddot{O}} + 3O^x_O \tag{6}$$

$$Sm_2O_3 \xrightarrow{2CeO_2} 2Sm'_{Ce} + V_{\ddot{O}} + 3O^x_O \tag{7}$$

Fig. 7(a and b) shows the temperature dependence of grain conductivity and grain boundary conductivity for $Ce_{0.8}Sm_{0.2-x}La_xO_{1.9}$ electrolytes, respectively, in the 200–450 °C temperature range. It can be seen that grain conductivity and grain boundary conductivity are higher

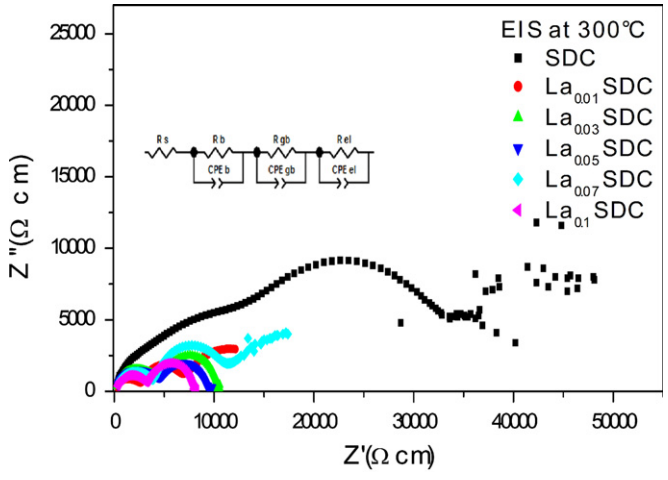

Fig. 6. Impedance spectra and equivalent circuit of $Ce_{0.8}Sm_{0.2-x}La_xO_{1.9}$ sintered at 1500 °C for 7 h at the measured temperature of 300 °C in air.

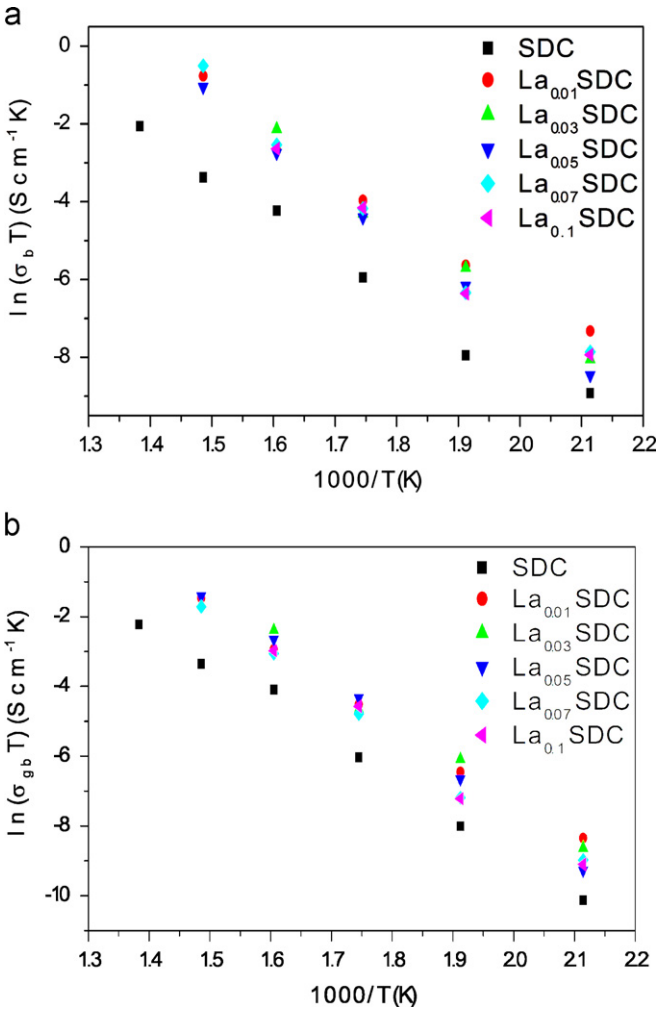

Fig. 7. (a) Temperature dependence of grain conductivity obtained for the.$Ce_{0.8}Sm_{0.2-x}La_xO_{1.9}$ electrolyte sintered at 1500 °C for 7 h. (b). Temperature dependence of grain boundary conductivity obtained for the $Ce_{0.8}Sm_{0.2-x}La_xO_{1.9}$ electrolyte sintered at 1500 °C for 7 h.

than the corresponding Sm singly-doped ceria conductivity, suggesting that a co-doping effect exists. Grain conductivity (σ_b) for all the samples is higher than the grain boundary conductivity (σ_{gb}). It can also be observed in Table 2 that the grain boundary activation energy is higher than the grain activation energy. This confirms the blocking effect of grain boundaries [19,28].

As reported in literature, the grain boundary resistance is created by the presence of contaminants and the depletion of oxygen vacancy concentrations in space charge layers [15,19,28]. As shown in Fig. 7(a), the ionic conductivity of grains increases with increasing lanthanum content up to 3 mol% For a higher concentration of La^{3+} ($y > 0.03$) said ionic conductivity decreases. This is probably due to the dissolution of La_2O_3 in the ceria. Dissolution of La^{3+} ions in a samarium-doped ceria sample will produce a higher activation energy and hence a lower conductivity. Li et al. [15] also proved that the improvement of grain conductivity for $Ce_{0.9}$ $(Sm_xNd_{1-x})_{0.1}O_{1.95}$ systems mostly lies on the improvement of ln σ_0.

Table 2
Activation energies and conductivity of $Ce_{0.8}Sm_{0.2-x}La_xO_{1.9}$ electrolytes.

Samples	Activation energy (eV)				Conductivity (10^{-2} S cm^{-1})
	E_b	E_{gb}	E_{tot}		σ_{tot} at 700 °C
	200–450 °C	200–450 °C	200–450 °C	500–700 °C	
SDC	0.83	0.94	0.84	0.96	1.19
$La_{0.01}$SDC	0.87	0.94	0.99	0.55	1.51
$La_{0.03}$SDC	0.97	1.02	1.09	0.77	3.80
$La_{0.05}$SDC	1.00	1.09	1.09	0.86	2.39
$La_{0.07}$SDC	1.00	1.02	1.03	0.75	2.23
$La_{0.1}$SDC	0.91	1.06	1.07	0.64	1.11

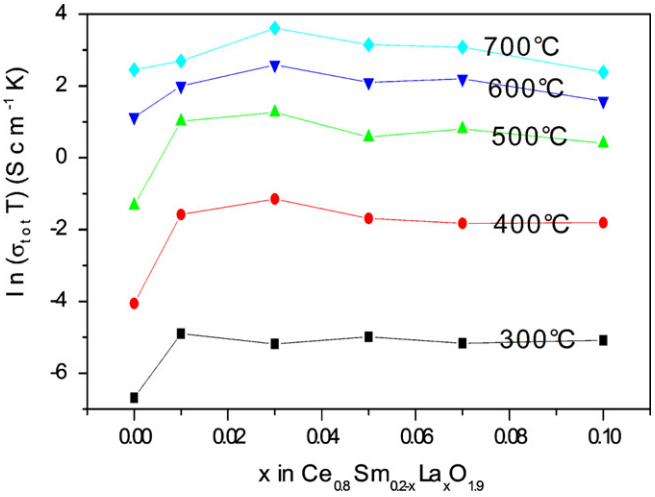

Fig. 8. Plot of the total conductivity as a function of the La content at different temperatures for the $Ce_{0.8}Sm_{0.2-x}La_xO_{1.9}$ series sintered at1500 °C for 7 h.

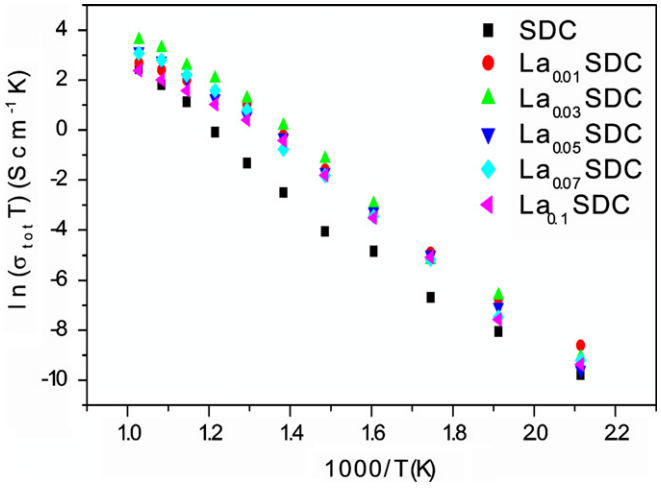

Fig. 9. Temperature dependence of total conductivity obtained for the $Ce_{0.8}Sm_{0.2-x}La_xO_{1.9}$ electrolyte sintered at 1500 °C for 7 h.

Fig. 8 shows the isothermal plots of total conductivity versus lanthanum content at different temperatures. The conductivity of $Ce_{0.8}Sm_{0.2-x}La_xO_{1.9}$ first increased ($x < 0.03$) and then decreased ($x > 0.03$) with Nd dopant content x. $Ce_{0.8}Sm_{0.17}La_{0.03}O_{1.9}$ exhibits the highest electrical conductivity throughout the whole temperature range, 250–700 °C. The observed conductivity of this composition was equal to 0.038 S cm^{-1} at 700 °C, which was higher than 0.0119 S cm^{-1} found for the single-doped ceria $Ce_{0.8}Sm_{0.2}O_{1.9}$ at 700 °C and also higher than what was reported in literature [29]. Moreover, the conductivity value was also higher than that of single-doped $Ce_{0.85}La_{0.15}O_{2-\delta}$ found in literature [21].We can once again see that the samarium single-doped sample (SDC) exhibits the smallest ionic conductivity throughout the entire temperature range (250–700 °C) studied.

As shown in Fig. 8, the difference between total conductivities of La_xSDC samples decreases with the increase of temperature. According to Cioateră et al. [27], this behavior might be due to an increase in the concentration of charge carriers arising from trivalent doping at high temperatures.

The total electrical conductivity at 700 °C and the activation energy values for two temperature regions are given in Table 2. It can be seen from Table 2 that the activation energy increases with increasing La dopant content x in the lower temperature ranges. This may be due to the formation of both, order clusters and local ordering [15]. However, the decrease of the activation energy at higher temperature ranges is due to the dopant-oxygen vacancy complex dissociating completely to free a dopant cation and oxygen vacancy, which is consistent with the observations of Ozdemir et al. [14]. This decrease is due to the presence of attractive interactions between dopant cations and oxygen vacancies [19,28].

Fig. 9 shows the Arrhenius plot of the total electrical conductivity for the samples with different lanthanum contents in the temperature range 250–700 °C. It can be seen that the addition of La improves the ionic conductivity. The $Ce_{0.8}Sm_{0.17}La_{0.03}O_{1.9}$ sample obviously possesses the highest total ionic conductivity, in consistency with Fig. 8.

As can be seen in Fig. 9, the Arrhenius plot shows a significant curve which is usually interpreted as a transition from associated to dissociated behavior of the defect cluster or complex. This curvature is observed at around

400–500 °C, and arises from the differences in the conduction mechanism due to the changes in the behaviors of the defect at low (200–450 °C) and high (500–700 °C) temperatures. Furthermore, the gradient change in the Arrhenius plot for the $Ce_{0.8}Sm_{0.2-x}La_xO_{1.9}$ compositions can be observed, and which has previously been found for numerous doped ceria solid solutions, such as $Ce_{1-x}Gd_xO_{2-\delta}$ [8], $Ce_{1-x}Sm_xO_{2-\delta}$ [20], $Ce_{1-x}Nd_xO_{2-\delta}$ [4], and $Ce_{1-x}Y_xO_{2-\delta}$ [10], and for co-doped ceria solid electrolytes too, including $Ce_{0.8}Sm_{0.1}Ln_{0.1}O_{1.9}$ [25], $Ce_{1-x}(Sm_{0.5}Nd_{0.5})_xO_\delta$[15] and $Sm_{x/2}Nd_{x/2}Ce_{1-x}O_{2-\delta}$ [30]. This means that is in the low temperature region, activation energy (E_a) equals the migration energy (E_{mg}) and the defect association energy (E_{as}), because the oxygen vacancy associated with the dopant is trapped on account of the association of defects to form defect complexes. Accordingly, both the association and migration energies of the system influence the conduction mechanism. But the high temperature region is only associated with the migration energy, because oxygen vacancies are assumed to be mobile [19,30,26]. It can also be noted that the difference between the total conductivities of $Ce_{0.8}Sm_{0.2-x}La_xO_{1.9}$ samples increases at high temperatures. At a low dopant concentration, most of the oxygen vacancies *V*ö are probably mobile while at high dopant concentrations, defect associations localized near the dopants begin to form at the expense of oxygen vacancies [27,31].

If the conductivity of the La0.1SDC compound (0.038 S/ cm) in this paper is compared to that prepared with citric acid-nitrate (0.0659 S/cm) [25], it can be seen that the preparation method affects the electrical properties.

4. Conclusions

Lanthanum (La) and samarium (Sm) co-doped ceria systems $Ce_{0.8}Sm_{0.2-x}La_xO_{1.9}$ ($x=0.00$, 0.01, 0.03, 0.05, 0.07 and 0.1) are successfully synthesized through the mechanical milling reaction method. Dense ceramics are obtained by sintering the pellets at 1500 °C for 7 h. The relative densities are over 93% of the theoretical density and these results are consistent with the SEM studies. The lattice parameter increases linearly with increasing La content. The ionic conductivity of co-doped ceria samples is higher than for singly-doped ceria. The $Ce_{0.8}Sm_{0.17}La_{0.03}O_{1.9}$ sample gave the highest conductivity value of 0.038 S cm^{-1} at 700 °C. These co-doped ceria materials can be used as possible electrolyte material for IT-SOFC applications.

Acknowledgments

This work was supported by the Ministry of Higher Education and Scientific Research of Tunisia. The author would also like to thank the language expert Nayua Abdelkefi for proofreading the manuscript.

References

[1] A. M-Hernandez, J. V-Castillo, L. Mogni, A. Caneiro, Thermal stability of $Ln_2NiO_{4+\delta}$ (Ln: La, Pr, Nd) and their chemical compatibility with YSZ and CGO solid electrolytes, International Journal of Hydrogen Energy 36 (2011) 15704–15714.
[2] N.T. Hart, N.P. Brandon, M.J. Day, N. Lapena-Rey, Functionally graded composite cathodes for solid oxide fuel cells, Journal of Power Sources 106 (2002) 42–50.
[3] B.C.H. Steele, Appraisal of $Ce_{1-y}GdyO_{2-y/2}$ electrolytes for IT-SOFC operation at 500 °C, Solid State Ionics 129 (2000) 95–110.
[4] I.E.L. Stephens, J.A. Kilner, Ionic conductivity of $Ce_{1-x}Nd_xO_{2-x/2}$, Solid State Ionics 177 (2006) 669–676.
[5] X. Li, Z. Feng, J. Lu, F. Wang, M. Xue, G. Shao, Synthesis and electrical properties of $Ce_{1-x}Gd_xO_{2-x/2}$ ($x=0.05$–0.3) solid solutions prepared by a citrate–nitrate combustion method, Ceramics International 38 (2012) 3203–3207.
[6] T. Karaca, T.G. Altıncekic, M.F. Oksuzomer, Synthesis of nanocrystalline samarium-doped CeO_2 (SDC) powders as a solid electrolyte by using a simple solvothermal route, Ceramics International 36 (2010) 1101–1107.
[7] S. Dikmen, P. Shuk, M. Greenblatt, Hydrothermal synthesis and properties of $Ce_{1-x}La_xO_{2-\delta}$. solid solutions, Solid State Ionics 126 (1999) 89–95.
[8] Z. Tianshu, P. Hing, H. Huang, J. Kilner, Ionic conductivity in the CeO_2_Gd_2O_3 system($0.05 \le Gd/Ce \le 0.4$) prepared by oxalate coprecipitation., Solid State Ionics 148 (2002) 567–573.
[9] S. Dikmen, P. Shuk, M. Greenblatt, H. Gocmez, Hydrothermal synthesis and properties of $Ce_{1-x}Gd_xO_{2-\delta}$ solid solutions, Solid State Sciences 4 (2002) 585–590.
[10] T.S. Zhang, J. Ma, H.T. Huang, P. Hing, Z.T. Xia, S.H. Chan, J.A. Kilner, Effects of dopant concentration and aging on the electrical properties of Y-doped ceria electrolytes, Solid State Sciences 5 (2003) 1505–1511.
[11] N. Jaiswal, N.K. Singh, D. Kumar, O. Parkash, Effect of strontium (Sr) doping on the conductivity of ceria, Journal of Power Sources 202 (2012) 78–84.
[12] P. Shuk, M. Greenblatt, M. Croft, Hydrothermal synthesis and properties of $Ce_{1-x}Eu_xO_{2-\delta}$ solid solutions, Journal of Alloys and Compounds 303–304 (2000) 465–471.
[13] H. Arai, T. Kunizaki, Y. Shimizu, T. Seiyama, Electrical properties of calcia-doped ceria with oxygen ion conduction, Solid State Ionics 20 (1986) 241–248.
[14] H. Özdemir, V. Sarıboga, M.A.F. Öksüzömer, M.A. Gürkaynak, Preparation and characterization of Ca–Sm–Ce mixed oxides via cellulose templating method for solid oxide fuel cell applications, Journal of Power Sources 219 (2012) 155–162.
[15] B. Li, Y. Liu, X. Wei, W. Pan, Electrical properties of ceria Co-doped with Sm^{3+} and Nd^{3+}, Journal of Power Sources 195 (2010) 969–976.
[16] H.C. Yao, Y.X. Zhang, J.J. Liu, Y.L. Li, J.S. Wang, Z.J. Li, Synthesis and characterization of Gd^{3+} and Nd^{3+} co-doped ceria by using citric acid–nitrate combustion method, Materials Research Bulletin 491 (2010).
[17] Y. Zheng, L. Wu, H. Gu, L. Gao, H. Chen, L. Guo., The effect of Sr on the properties of Y-doped ceria electrolyte for IT-SOFCs, Journal of Alloys and Compounds 486 (2009) 586–589.
[18] V.P. Kumar, Y.S. Reddy, P. Kistaiah, G. Prasad, C.V. Reddy., Thermal and electrical properties of rare-earth co-doped ceria ceramics, Materials Chemistry and Physics 112 (2008) 711–718.
[19] S. Ramesh, V.P. Kumar, P. Kistaiah, C.V. Reddy, Preparation, characterization and thermo electrical properties of co-doped $Ce_{0.8-x}Sm_{0.2}Ca_xO_{2-\delta}$ materials, Solid State Ionics 181 (2010) 86–91.
[20] H. Yahiro, Y. Eguchi, K. Eguchi, H. Arai, Oxygen ion conductivity of the ceria- samarium oxide system with fluorite structure, Journal of Applied Electrochemistry 18 (1988) 527–531.
[21] Y. Zheng, Y. Shi, H. Gu, L. Gao, H. Chen, L. Guo., La and Ca co-doped ceria-based electrolyte materials for IT-SOFCs, Materials Research Bulletin 44 (2009) 1717–1721.

[22] M. Mogensen, N.M. Sammes, G.A. Tompsett, Physical, chemical and electrochemical properties of pure and doped ceria, Solid State Ionics 129 (2000) 63–94.

[23] S. Dikmen, Effect of co-doping with Sm^{3+}, Bi^{3+}, La^{3+}, and Nd^{3+} on the electrochemical properties of hydrothermally prepared gadolinium-doped ceria ceramics, Journal of Alloys and Compounds 491 (2010) 106–112.

[24] F.Y. Wang, S. Chen, S. Cheng., Gd^{3+} and Sm^{3+} co-doped ceria based electrolytes forintermediate temperature solid oxide fuel cells., Electrochemistry Communications 6 (2004) 743–746.

[25] M. Kahlaoui, S. Chefi, A. Inoubli, A. Madani, C. Chefi, Synthesis and electrical properties of co-doping with La^{3+}, Nd^{3+}, Y^{3+}, and Eu^{3+} citric acid–nitrate prepared samarium-doped ceria ceramics, Ceramics International (2012). http://dx.doi.org/10.1016/j.ceramint.2012.10.230.

[26] H. Li, C. Xia, M. Zhu, Z. Zhou, G. Meng, Reactive $Ce_{0.8}Sm_{0.2}O_{1.9}$ powder synthesized by carbonate coprecipitation: sintering and electrical characteristics, Acta Materialia 54 (2006) 721–727.

[27] N. Cioateră, V. Pârvulescu, A. Rolle, R.N. Vannier, Effect of strontium addition on europium-doped ceria properties, Solid State Ionics 180 (2009) 681–687.

[28] N. Jaiswal, S. Upadhyay, D. Kumar, Om Parkash, Ionic conductivity investigation in lanthanum (La) and strontium (Sr) co-doped ceria system, Journal of Power Sources 222 (2013) 230–236.

[29] X. Sha, Z. Lu, X. Huang, J. Miao, L. Jia, X. Xin, W. Su, Preparation and properties of rare earth co-doped $Ce_{0.8}Sm_{0.2-x}Y_xO_{1.9}$ electrolyte materials for SOFC, Journal of Alloys and Compounds 424 (2006) 315–321.

[30] S. Omar, E.D. Wachsman, J.C. Nino, Higher conductivity Sm^{3+} and Nd^{3+} co-dopedceria-based electrolyte materials, Solid State Ionics 178 (2008) 1890–1897.

[31] R.A. M-Lozano, S.M. Montemayor, K.P. Padmasree, A.F. Fuentes, Effect of Ca^{2+} or Mg^{2+} additions on the electrical properties of Yttria doped ceria electrolyte system, Journal of Alloys and Compounds 525 (2012) 184–190.